Synthesis, Structure, and Magnetic Properties of a Tris[3-(2-pyridyl)-1,2,4-triazole]iron(II) Spin-Crossover Complex

Arno F. Stassen,[a] Matthijs de Vos,[a] Petra J. van Koningsbruggen,[b] Franz Renz,[b] Jürgen Ensling,[b] Huub Kooijman,[c] Anthony L. Spek,[d][+] Jaap G. Haasnoot,*[a] Philipp Gütlich,[b] and Jan Reedijk[a]

Dedicated to Professor Heinrich Vahrenkamp on the occasion of his 60th birthday

Keywords: Spin crossover / Iron / Magnetic properties / Moessbauer spectroscopy / N ligands

The synthesis and characterization of tris[3-(pyridin-2-yl)-1,2,4-triazole]iron(II) bis(tetrafluoroborate), obtained from the reaction of 3-(pyridin-2-yl)-1,2,4-triazole (Hpt) and hexaaquairon(II) tetrafluoroborate, $[Fe(H_2O)_6](BF_4)_2$, is described, together with its crystal structures at two temperatures. X-ray crystallographic parameters are as follows: $[Fe(Hpt)_3](BF_4)_2 \cdot nH_2O$ ($n \approx 2$) at 250 K: orthorhombic space group *Pbam*, a = 15.8068(18) Å, b = 17.2800(14) Å, c = 21.215(2) Å, V = 5794.7(10) Å^3, and Z = 8. $[Fe(Hpt)_3](BF_4)_2 \cdot nH_2O$ ($n \approx 2$) at 95 K: orthorhombic space group *Pbam*, a = 15.7080(12) Å, b = 17.1023(16) Å, c = 21.006(2) Å, V = 5643.1(9) Å^3, and Z = 8. The Fe^{II} ions are (at both temperatures) octahedrally surrounded in a *mer*-configuration. The complex has been subjected to both ^{57}Fe Mössbauer spectroscopy and magnetic susceptibility measurements. The ^{57}Fe Mössbauer spectrum shows the presence of two different iron(II) sites. The high-spin fraction vs. T curve of the crossover, obtained by SQUID measurements, is gradual and without hysteresis, with $T_{1/2}$ = 135 K.

Introduction

Nowadays there is increasing interest in new bistable iron(II) spin-crossover compounds.[1,2] A variety of iron(II) compounds are known to show a transition from the high-spin state [HS, $S = 2$, $^5T_{2g}$ (O_h)] to the low-spin state [LS, $S = 0$, $^1A_{1g}$ (O_h)] on cooling.[2−4]

Iron(II) compounds incorporating substituted 1,2,4-triazole ligands have been found to undergo spin transition. In several cases, hysteresis effects and rather high transition temperatures have been found.[5−23] Generally speaking, when dealing with linear polynuclear Fe^{II} compounds of 1,2,4-triazole ligands, the spin-crossover behaviour is abrupt and may show hysteresis,[5,7,11−16,19,21,22,24,25] but this is not the case for shorter oligomers.[26−28] For mononuclear 1,2,4-triazole-containing iron(II) spin-crossover systems, the spin crossover has always been found to be gradual and without any hysteresis.[9,10,18,29,30]

^{57}Fe Mössbauer spectroscopy studies on $[Fe(Hpt)_3](Anion)_2(Solvent)_x$ [Hpt = 3-(pyridin-2-yl)-1,2,4-triazole (see Figure 1); Anion = Cl^-, ClO_4^-, PF_6^-, BF_4^-; Solvent = ethanol, water] and $[Fe(H3mpt)_3](Anion)_2(Solvent)_x$ [H3Mpt = 3-methyl-5-(pyridin-2-yl)-1,2,4-triazole; Anion = ClO_4^-, PF_6^-; Solvent = water] have been reported by Stupik et al.[9,10] and by Sugiyarto et al.[31] Clearly, these mononuclear compounds exhibit continuous Fe^{II} spin-crossover behaviour. The Fe^{II} ion resides in a six-nitrogen environment made up of three bidentate chelating 3-(pyridin-2-yl)-1,2,4-triazole ligands coordinating through N4 of the 1,2,4-triazole and the pyridine N. The asymmetric nature of the bidentate ligand may lead to the formation of FeL_3 units having *facial* or *meridional* geometry. Both Stupik and Sugiyarto observed[9,10,31] that the spin transition was affected by the presence of different solvent molecules. This contributes to the complicated spin-crossover behaviour evident from the ^{57}Fe Mössbauer spectra. They also observed two different iron(II) high-spin sites in the hydrated BF_4^- complex, but did not mention the ratio between the two sites. In addition, Sugiyarto et al.[31] reported comparable observations for the hydrated BF_4^- and ClO_4^- iron(II) tris[3-(pyridin-2-yl)-1,2,4-triazole] compounds.

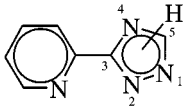

Figure 1. Structure of 3-(pyridin-2-yl)-1,2,4-triazole (Hpt)

[a] Leiden Institute of Chemistry, Gorlaeus Laboratories, Leiden University,
P.O. Box 9502, NL-2300 RA Leiden, The Netherlands
Fax: (internat.) +31−715274671
E-mail: haasnoot@chem.leidenuniv.nl
[b] Institut für Anorganische Chemie und Analytische Chemie, Universität Mainz,
Staudingerweg 9, D-55099 Mainz, Germany
[c] Bijvoet Center for Biomolecular Research, Utrecht University,
Padualaan 8, NL-3584 CH Utrecht, The Netherlands
E-mail: a.l.spek@chem.uu.nl
[+] Address correspondence pertaining to crystallographic studies to this author.

  1434−1948/00/1010−2231 $ 17.50+.50/0

However, these results have not yet been satisfactorily explained, and hence a further study on this interesting class of compounds was undertaken.

In this paper, the synthesis, crystal structures at 250 K and 95 K, and physical properties of the iron(II) Hpt coordination complex of the anion BF_4^- are described in detail.

Results and Discussion

Structure of the Complex

X-ray crystal structure analyses have been carried out at two temperatures, i.e. at 250 K, where the complex is almost completely high spin, and at 95 K, which is below the transition temperature and hence most of the iron(II) ions participating in the spin-crossover behaviour are in the low-spin state. The molecular structure showing the atomic numbering scheme is depicted in Figure 2, while relevant bond length and bond angle information is given in Table 1 and Table 2. At both temperatures, the space group is *Pbam* with $Z = 8$. The asymmetric unit contains one $Fe(Hpt)_3$ moiety. Structural analysis of the complex shows that at both temperatures the iron(II) is octahedrally surrounded by three Hpt ligands, which bind through N2 of the pyridine ring and N4 of the triazole ring in a *mer* configuration.

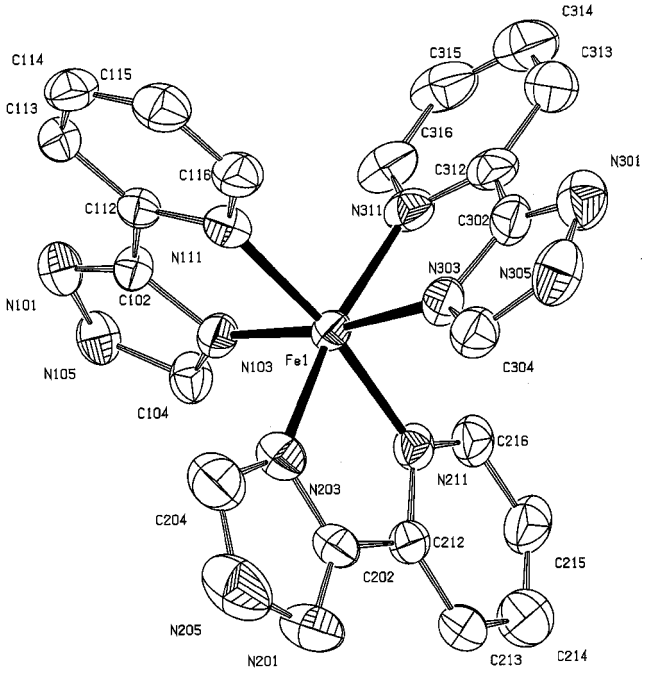

Figure 2. Displacement ellipsoid plot drawn at a 50% probability level of the complex cation $[Fe(Hpt)_3](BF_4)_2 \cdot nH_2O$ at 95 K

Table 1. Relevant bond lengths in $[Fe(Hpt)_3](BF_4)_2 \cdot nH_2O$ at 95 K and 250 K

Bond	Length at 95 K [Å]	Length at 250 K [Å]
Fe−N(103)	2.003(3)	2.127(4)
Fe−N(203)	2.011(3)	2.160(4)
Fe−N(303)	2.009(3)	2.154(4)
Fe−N(111)	2.051(3)	2.202(3)
Fe−N(211)	2.041(3)	2.199(4)
Fe−N(311)	2.047(3)	2.229(4)

Table 2. Important angles in $[Fe(Hpt)_3](BF_4)_2 \cdot nH_2O$ at 95 K and 250 K

Bond angle	Angle at 95 K	Angle at 250 K
N(103)−Fe−N(303)	171.19(13)	164.82(14)
N(111)−Fe−N(211)	171.04(12)	166.71(12)
N(203)−Fe−N(311)	169.33(12)	163.95(17)
N(103)−Fe−N(111)	80.68(12)	77.13(13)
N(203)−Fe−N(211)	80.17(13)	77.00(15)
N(303)−Fe−N(311)	80.33(13)	75.53(15)
N(103)−Fe−N(203)	96.25(13)	100.75(16)
N(103)−Fe−N(211)	92.05(12)	92.43(13)
N(103)−Fe−N(311)	93.20(12)	93.62(15)
N(111)−Fe−N(203)	95.08(12)	96.67(15)
N(111)−Fe−N(303)	93.24(12)	92.74(13)
N(111)−Fe−N(311)	91.31(12)	93.45(14)
N(203)−Fe−N(303)	90.77(13)	91.53(15)
N(211)−Fe−N(303)	94.41(12)	99.04(13)
N(211)−Fe−N(311)	94.57(12)	95.42(14)

Because of rotational and positional disorder of the tetrafluoroborate and water molecules, it was not possible to determine any positional parameters for these molecules. This disorder suggests the absence of hydrogen bonding. This is surprising, because both N1 and N2 of the triazole ring can form hydrogen bonds, either in amino or imino form.[32]

Comparison of the bond angles of the N−Fe−N axes at the two temperatures shows that at low temperature the angles are closer to 180°, as would be expected for a $^1A_{1g}$ octahedral structure. The N−Fe−N angles involving the nitrogen atoms on different axes are also closer to those of a regular octahedron at 95 K than at 250 K. The ligand bite angles increase from 75.53−77.13° at 250 K to 80.17−80.86° at 95 K. The other nonlinear N−Fe−N angles decrease from 91.53−100.75° (average 95.1°) at 250 K to 90.77−96.25° (average 93.4°) at 95 K. Considering that at this temperature 35% of the complexes are still in the high-spin state, the actual angles in the low-spin complex will be even closer to 90°.

The Fe−N bond length contracts by approximately 0.15 Å on cooling to 95 K. These observations can be rationalized as follows. For iron(II) complexes surrounded by neutral ligands, Equation (1) holds, where μ is the dipole moment of the ligand and r the average metal−ligand distance.[1]

$$10Dq \approx \frac{\mu}{r^6} \quad (1)$$

From this equation, Equation (2) can be derived.

$$\frac{10Dq^{LS}}{10Dq^{HS}} = \left(\frac{r_{HS}}{r_{LS}}\right)^6 \approx 1.74 \quad (2)$$

The value for an iron(II) spin-crossover complex is normally ca. 1.74. The value obtained by applying Equation (2) in the case of $[Fe(Hpt)_3](BF_4)_2 \cdot n\,H_2O$ is lower than 1.74, specifically 1.57. The difference between the calculated and measured values arises from the fact that at both temper-

atures not all the iron(II) ions are in the same spin state. From magnetic and Mössbauer measurements, it has been concluded that at 95 K a residue of 36.1% high-spin and at 250 K a residue of 2.5% of low-spin iron(II) ions is present. The actual Fe−N bond length for a pure low-spin state will be closer to 2.00 Å, and using this value in Equation 2 would generate the expected dipole moment.

Because the contribution to the structure factors associated with the counter ions and solvent was taken into account using the SQUEEZE procedure as incorporated in PLATON,[33] no exact molecular formula could be determined from the crystal structure. However, considering the number of electrons associated with the counterions and solvent in conjunction with the elemental analysis, the molecular formula could be calculated. Assuming that only cations of the formula $[Fe(Hpt)_3]^{2+}$, anions BF_4^-, and water were present, the molecular formula $[Fe(Hpt)_3](BF_4)_2 \cdot nH_2O$, $n = 2$, was derived.

The stability of the complex was tested by heating it for several hours at 50 °C and by storing it in vacuo for one day. Under neither conditions were the elemental analysis or magnetic susceptibility affected. Thus, despite the fact that the water molecules are seemingly not involved in strong hydrogen bonding, they are not readily removed from the complex.

^{57}Fe Mössbauer Spectroscopic Measurements

^{57}Fe Mössbauer spectra were recorded at temperatures of 300 K, 205 K, 150 K, 80 K, 32 K, 10 K, and 4.2 K. A representative selection of the spectra is shown in Figure 3. Least-squares-fitted parameters are listed in Table 3. In all the spectra, three doublets have been assigned. Of these, one is characteristic of Fe^{II} in the low-spin state, while the other two are characteristic of Fe^{II} in the high-spin state.[34] We shall refer to the high-spin doublet with the larger quadrupole splitting as HSa, and to the other as HSb. Stupik[9,10] and Sugiyarto[31] also detected a second high-spin site, but it is not clear as to whether the site they detected was identical to HSb (these authors did not analyse the spectra in more detail). Schreiner[29] also detected a second high-spin site in $[Fe(Hpt)_3](BF_4)_2 \cdot H_2O/EtOH$, to the extent of 7% at 100 K (31% at 300 K), which was reported to behave similarly as that found in the present work. The area fraction of the HSb site is only 6% at 205 K and decreases to 3% at 4.2 K, which is close to the experimental limit. Its corresponding Fe^{II} low-spin state doublet probably coincides with the aforementioned major low-spin doublet. The molar ratios of the molecules in the spin states can be derived from the area fractions by taking equal Mössbauer−Lamb factors for the low-spin and high-spin states.[35,36]

At 300 K, a pure high-spin state doublet is present (unresolved HSa and HSb). At 205 K, a low-spin doublet of weak intensity is visible, associated with 8% of the ions. This low-spin doublet clearly increases in intensity on going from 205 to 80 K (from 8% to 67%), while the doublet associated with the HSa site gradually diminishes from 86% at 205 K to 30% at 80 K. At the latter temperature, the spin

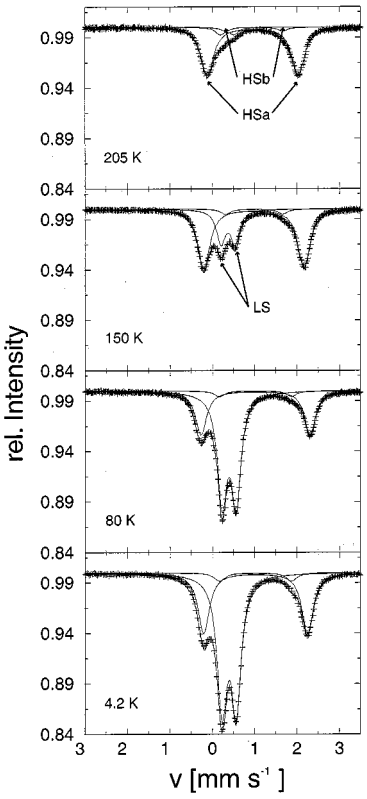

Figure 3. ^{57}Fe Mössbauer spectral measurements at 205, 150, 80, and 4.2 K

crossover is almost complete. Further cooling to 4.2 K results only in an additional 2% increase in the intensity of the low-spin doublet to 69%. The distribution of high-spin and low-spin species found at the measured temperatures is in agreement with the magnetic measurements.

When a spin-crossover compound is cooled very rapidly, i.e. quenched, it is possible that high-spin ions are unable to relax to the low-spin state, but remain thermally spin trapped in the metastable high-spin state.[37−39] This phenomenon is called thermal spin trapping. Mössbauer spectra measured after rapid cooling, i.e. by taking a sample at 300 K and placing it in a cryostat at 4.2 K, revealed that a fraction of the iron(II) ions, approximately 6%, is trapped in the high-spin state (see Table 3). It is mainly the HSb site that exhibits the spin state trapping.

The presence of a second high-spin site (HSb) indicates a different local surrounding from the majority (HSa), arising from the distribution of the solvent and anions.

Magnetic Susceptibility Measurements

Figure 4 shows the product of χT and T for $[Fe(Hpt)_3](BF_4)_2 \cdot 2\,H_2O$, where χT is the molar magnetic susceptibility, recorded in the temperature range 4−325 K as a function of temperature T. The curve provides evidence for $S = 2$ (HS) ⇄ $S = 0$ (LS) spin-crossover behaviour. At room temperature, all iron(II) ions are in the high-spin state ($\chi T = 3.52$ cm^{3}Kmol^{-1}). Below 75 K, the value of χT falls to 0.72 cm^{3}Kmol^{-1}. This indicates the presence of a signi-

Table 3. Least-squares fitted Mössbauer parameters for $[Fe(Hpt)_3](BF_4)_2 \cdot 2\,H_2O$

T (K)	δ(LS)[a] (mm s^{-1})	ΔE_Q(LS) (mm s^{-1})	Γ(LS) (mm s^{-1})	A_{LS} (%)	δ(HS) (mm s^{-1})	ΔE_Q(HS) (mm s^{-1})	Γ(HS) (mm s^{-1})	A_{HS} (%)	δ(HS) (mm s^{-1})	ΔE_Q(HS) (mm s^{-1})	Γ(HS) (mm s^{-1})	A_{HS} (%)
205	0.34(1)	0.32(1)	0.15(1)	8	0.95(0)	2.14(1)	0.25(1)	86	1.10(1)	1.35(1)	0.19(1)	6
150	0.37(1)	0.33(1)	0.15(1)	27	0.98(1)	2.36(1)	0.25(1)	68	1.10(1)	1.35(1)	0.19(1)	5
80	0.39(1)	0.33(1)	0.16(1)	67	1.02(1)	2.57(1)	0.23(1)	30	1.13(1)	1.70(1)	0.20(1)	3
32	0.40(1)	0.33(1)	0.16(1)	69	1.03(1)	2.54(1)	0.22(1)	28	1.13(1)	1.70(1)	0.20(1)	3
10	0.40(1)	0.33(1)	0.16(1)	69	1.03(1)	2.45(1)	0.20(1)	28	1.13(1)	1.70(1)	0.20(1)	3
4.2	0.40(1)	0.33(1)	0.16(1)	69	1.03(1)	2.47(1)	0.20(1)	28	1.13(1)	1.75(1)	0.20(1)	3
After quenching from 300 K (approx. 100 K s^{-1})												
4.2	0.40(1)	0.33(1)	0.16(1)	63	1.04(1)	2.45(1)	0.20(1)	29	1.13(1)	1.80(1)	0.20(1)	7

[a] δ = isomer shift, ΔE_Q = quadrupole splitting, Γ = line width, A_{HS} = area fraction of the HS doublets. Statistical standard deviations are given in parentheses.

ficant residue of high-spin iron(II) ions, as is also evident from the low-temperature Mössbauer spectrum. The spin transition is very gradual, with $T_{1/2}$ = 135 K. The parameter $T_{1/2}$ is defined as the temperature in a thermally driven spin equilibrium at which, for the iron(II) ions involved in spin transition, the amounts of high-spin and low-spin molecules are equal. The entire measurement required 5 h 45 min, corresponding to a heating rate of approximately 1.1 $Kmin^{-1}$ in steps of 2.5 K.

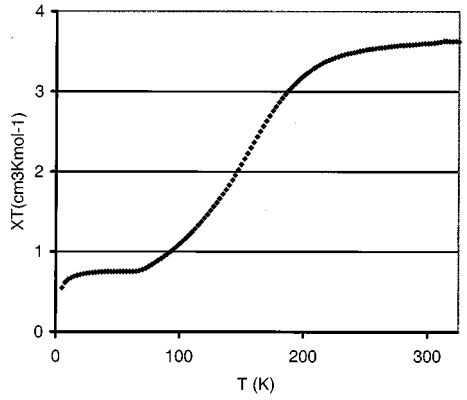

Figure 4. Plot of χT vs. T for $[Fe(Hpt)_3](BF_4)_2 \cdot 2\,H_2O$

The spin transition takes place without hysteresis. Furthermore, the spin-crossover behaviour is easily detected, since the compound is highly thermochromic. On cooling to 77 K, its colour changes from yellow to deep purple.

Figure 5 shows the γ_{HS} vs. T curve plotted over the temperature range 4−320 K. The high-spin molar fraction γ_{HS} was deduced from the ^{57}Fe Mössbauer data area fractions by taking equal Mössbauer−Lamb factors for low-spin state and high-spin state doublets.[35,36] It may be assumed from the Mössbauer measurements that below 80 K 30% of the high-spin sites are not involved in the spin-crossover process. This makes it possible to simulate the spin-crossover curve using Equation (3), which is derived from the regular solution model.[40]

$$\ln\left[\frac{1-\gamma_{HS}}{\gamma_{HS}}\right] = \frac{\Delta H + \Gamma(1-2\gamma_{HS})}{RT} - \frac{\Delta S}{R} \qquad (3)$$

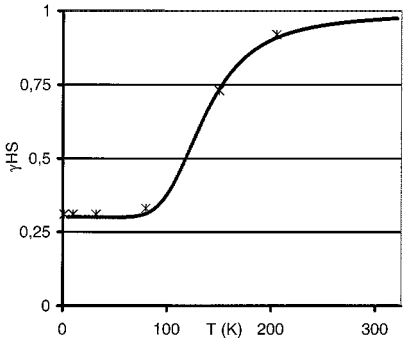

Figure 5. Fitted high-spin molar fraction, based on Mössbauer data, vs. T for $[Fe(Hpt)_3](BF_4)_2 \cdot 2\,H_2O$ (* = actual Mössbauer measurements)

In Equation (3), R is the molar gas constant, ΔH is the enthalpy change, and ΔS is the entropy change associated with the spin crossover. Least-squares fitting leads to ΔH = 6.4 kJ mol^{-1}, ΔS = 47 J K^{-1} mol^{-1}, and a mean-field interaction parameter Γ smaller than 0.1 kJ mol^{-1}. The spin crossover may be considered as being almost non-cooperative.[1,41]

Complexes of hexaaquairon(II) tetrafluoroborate with 3-(pyridin-2-yl)-1,2,4-triazole have been prepared in aqueous solutions at pH 7 to 14. The resulting complexes all exhibit identical spin-crossover behaviour and also give identical elemental analysis results. This excludes the presence of the deprotonated ligand (pt^-).

Ligand-Field Spectroscopy

The ligand-field spectrum of the present complex was measured in the diffuse reflection mode at room temperature and at liquid-nitrogen temperature. The $^5T_2 \rightarrow {}^5E$ transition is seen at 850 nm (11.765 cm^{-1}), while the $^1A_1 \rightarrow {}^1T_1$ transition appears at 530 nm (18.868 cm^{-1}). These values are in the regions normally observed for the corresponding d−d transitions in spin-crossover behaviour materials.[1]

Conclusion

In this paper, the spin-crossover complex tris(Hpt)Fe^{II} with tetrafluoroborate as anion has been reported. This complex is formed as the *meridional* isomer, just as the previously[9,10] studied $[Fe(Hpt)_3](ClO_4)_2 \cdot (Solvent)_x$. Bidentate coordination by the Hpt ligand takes place through N4 of the 1,2,4-triazole and the pyridine N. Details of the X-ray structure determination concerning the location of the tetrafluoroborate and water cannot be reported owing to high positional and rotational disorder of the counterion and solvent. The transition temperature $T_{1/2}$ has been determined as 135 K.

During the spin transition, the geometry of the complex does not change significantly. The average $Fe^{II}-N$ bond length decreases by approximately 0.15 Å. The average N−Fe−N bond angles become closer to those of an ideal octahedron on going from the high-spin to the low-spin state.

In the Mössbauer spectrum, two high-spin iron(II) sites with different populations are observed, with the HSa site clearly showing spin-crossover behaviour. Although a suitably intense doublet associated with the low-spin state is observed, it is not possible to determine whether only one low-spin site is present or whether the signals of two different sites are overlapping. The weak intensity HSb site is at the experimental limit of detection, hence no further conclusions can be made concerning the spin-crossover behaviour at this site. On rapid cooling, a small fraction of the high-spin ions can be thermally trapped in a metastable high-spin state.

It is difficult to compare these results with previously published observations on the $[Fe(Hpt)](BF_4)_2 \cdot 2H_2O$ complex.[9,10,31] These authors also noticed two types of high-spin site, but the data were not analysed further.

The disorder of the solvent molecules and counterions found in the crystal structure gives an indication that neither are involved in hydrogen bonding to the triazole rings of the Hpt ligands. Moreover, the distance between the nitrogens of the triazole ring and the electron density of the counterions and water molecules is too great for hydrogen bonding. The water molecules are nevertheless strongly bound to the complex and cannot be easily removed.

Approximately 30% of the Fe^{II} ions do not participate in the thermal spin transition. It is possible that the distribution of water molecules in the crystal lattice is responsible for this. In the almost identical system $[Fe(Hpt)_3](BF_4)_{1.2}(SO_4)_{0.4} \cdot 3H_2O$,[42] the spin transition does not have an associated high-spin residue at low temperature. It is known that in a few systems the solvent molecules are essential for the spin transition.[43,44] It seems likely that in the present system, due to a non-uniform distribution of water molecules in the lattice, some Fe^{II} ions remain in the high-spin state.

A small proportion (6%) of the iron(II) ions (HSb) experience a different coordination than that described in this article. There are several possibilities for the different coordination of HSb. One explanation is that the ligand is coordinated to the iron(II) through N2 of the triazole ring instead of N4. This would lead to a difference in the coordination sphere and hence in the Mössbauer spectrum; unfortunately, the difference that such a coordination would cause in the structural analysis is smaller than the experimental error. A further possibility is that the deprotonated ligand (pt^-) is present. In this case, 6% of the iron(II) ions would be surrounded by a deprotonated pt^- ligand and have only one tetrafluoroborate counterion in their coordination spheres. However, crystallization experiments at high pH (from 7 to 14) produced materials giving identical results in elemental analysis and susceptibility measurements. Therefore, this possibility can be excluded. A third possibility is that 6% of the crystals have the *facial* orientation. This different coordination could lead to a difference in both the ligand field and quadrupole splitting. In the *mer*-isomer, the three ligands are magnetically non-equivalent, whereas in the *fac*-isomer, the three ligands are magnetically equivalent as this isomer possesses a C_3-axis of symmetry.[45]

Both the first and third options are feasible. Triazole is known to be able to coordinate through N2 as well as through N4,[7,21,26] while both *fac*- and *mer*-isomers of (pyridin-2-yl)-1,2,4-triazole complexes are known.[31,45] Both the linkage and geometrical isomerism will cause a change in ligand field. Whether this variation is sufficiently large to be observed by Mössbauer spectroscopy remains uncertain.

Experimental Section

General Remarks: Ligand-field spectra of the solid were obtained on a Perkin−Elmer Lambda 900 spectrophotometer in the 2000−200 nm range using the diffuse reflectance technique, with MgO as a reference.

Magnetic susceptibilities were measured in the temperature range 5−325 K on a Quantum Design MPMS-5S SQUID operating at 0.1 Tesla. Data were corrected for magnetization of the sample holder and diamagnetic contributions, which were estimated using Pascal constants ($\chi_D = -2.85 \cdot 10^{-4}$ cm^3mol^{-1}).[46]

^{57}Fe Mössbauer spectra of the polycrystalline compound $[Fe(Hpt)_3](BF_4)_2 \cdot 2H_2O$ were recorded using a conventional spectrometer with the sample placed in a helium cryostat allowing variation of the temperature between 4 K and 300 K. As the source, ^{57}Co in rhodium at 293 K was used. The data were evaluated using the programs MOSFUN[35] and EFFI.[36] The high-spin molar fraction was estimated from the area fractions by taking equal Mössbauer−Lamb factors for low-spin and high-spin states.

Preparation of the Compounds: All chemicals were obtained commercially in adequately pure states. The ligand Hpt was synthesized from 2-cyanopyridine, hydrazine monohydrate, and formic acid according to the method described in literature.[32,47] Hpt: $C_7H_6N_4$ (146.2): calcd. C 57.53, H 4.14, N 38.33; found C 56.68, H 4.65, N 38.63.

$[Fe(Hpt)_3](BF_4)_2 \cdot 2H_2O$ was prepared under argon atmosphere by dissolving $[Fe(H_2O)_6](BF_4)_2$ (0.34 g, 1 mmol) and Hpt (0.44 g, 3 mmol) in hot, deoxygenated water (20 mL), to yield a clear brown solution. On standing in a closed flask at room temperature for

Table 4. Crystallographic data for $[Fe(Hpt)_3](BF_4)_2 \cdot nH_2O$ at 95 K and 250 K

Compound	T = 95 K	T = 250 K
	Crystal data	
Formula[a]	$C_{21}H_{18}FeN_{12} \cdot 2BF_4 \cdot 2H_2O$	$C_{21}H_{18}FeN_{12} \cdot 2BF_4 \cdot 2H_2O$
Molecular weight[a]	703.94	703.94
Crystal system	Orthorhombic	Orthorhombic
Space group	*Pbam* (no. 55)	*Pbam* (no. 55)
a [Å]	15.7080(12)	15.8068(18)
b [Å]	17.1023(16)	17.2800(14)
c [Å]	21.006(2)	21.215(2)
V [Å^3]	5643.1(9)	5794.7(10)
D_{calcd} [g cm^{-3}][a]	1.6572(2)*	1.6138(2)*
D_{obsd} [g cm^{-3}]		1.68
Z (mononuclear units)	8	8
$F(000)$ [a]	2848	2848
μ [mm^{-1} [Mo-K_α][a]	0.66	0.64
Crystal colour	red-brown	yellow-brown
	Data collection	
θ_{min}, θ_{max} [deg.]	1.6, 25.25	1.6, 25.25
X-ray exposure [h]	4	2
Data set	−18:18, −20:20, −25:25	−18:14, −20:16, −25:17
Total data	44707	22091
Total unique data	5273	5337
R_{int}	0.0907	0.0541
R_σ	0.0395	0.0552
	Refinement	
No. of refined params.	307	307
Final $R1$[b]	0.0681 [4433 $I > 2\sigma(I)$]	0.0740 [3766 $I > 2\sigma(I)$]
Final $wR2$[c]	0.1587	0.2039
Goodness of Fit	1.140	1.041
w^{-1}[d]	$\sigma^2(F^2) + (0.462P)^2 + 11.59P$	$\sigma^2(F^2) + (0.00755P)^2 + 13.51P$
$(\Delta/\sigma)_{av}$, $(\Delta/\sigma)_{max}$	<0.001, <0.001	<0.001, <0.001
Min. and max. residual density [e Å^{-3}]	−0.36, 0.36	−0.35, 0.33

[a] Including disordered anion and solvent contributions. − [b] $R1 = \Sigma \mid |F_o| - |F_c| \mid / \Sigma |F_o|$. − [c] $wR2 = \{\Sigma[w(F_o^2 - F_c^2)^2] / \Sigma[w(F_o^2)^2]\}^{1/2}$. − [d] $P = [\mathrm{Max}(F_o^2, 0) + 2F_c^2]/3$.

a few days, clear yellow block-shaped crystals were deposited. − $[Fe(Hpt)_3](BF_4)_2 \cdot 2\,H_2O$ (703.9): calcd. C 35.83, H 3.15, N 23.88, F 21.59; found C 35.93, H 3.32, N 23.9, F 19.6.

Crystal Structure Determination of $[Fe(Hpt)_3](BF_4)_2$: A single crystal of dimensions 0.10 × 0.15 × 0.30 mm was mounted on a Lindemann glass capillary and placed in the cold nitrogen stream of the diffractometer. Data were collected on an Enraf−Nonius KappaCCD diffractometer on a rotating anode (Mo-K_α radiation, graphite monochromator, λ = 0.71073 Å, Lp correction, no absorption correction). Two data sets were recorded from this crystal, one at T = 95 K and one at T = 250 K. Structure determination revealed that the only geometrical differences between these structures were those related to the spin transition. Since the data for the 250 K structure were rather poor due to crystal deterioration, an additional data set was collected on a second crystal of dimensions 0.20 × 0.35 × 0.35 mm. Geometric data pertaining to the two structures measured at 250 K proved to be equal within experimental error. The data for the 250 K structure reported here refer to the second data set. Pertinent data relating to the structure determinations are collected in Table 4. The structures were solved by direct methods using SHELXS-86.[48] Refinement on F^2 was performed with SHELXL-97.[49] The hydrogen atoms were included in the refinement in calculated positions riding on their carrier atoms. The non-hydrogen atoms were refined with anisotropic thermal parameters. The hydrogen atoms were refined with a fixed isotropic displacement parameter related to the value of the equivalent isotropic displacement parameter of their carrier atoms. The BF_4 counterions were found to be disordered and located in a region also containing disordered solvent molecules, probably water. The contribution to the structure factors associated with counterions and solvent was taken into account using the SQUEEZE procedure as incorporated in PLATON.[33] A total of 840 e were found in a volume of 1800 Å^3, equally distributed between two symmetry-related cavities. Neutral atom scattering factors and anomalous dispersion corrections were taken from the International Tables for Crystallography.[50] Geometrical calculations and the generation of illustrations were performed with PLATON.[33]

Crystallographic data (excluding structure factors) for the structures reported in this paper have been deposited with the Cambridge Crystallographic Data Centre as supplementary publication nos. CCDC-140484/140485. Copies of the data can be obtained free of charge on application to the CCDC, 12 Union Road, Cambridge CB2 1EZ, U.K. [Fax: (internat.) +44 (0)1223/336033; E-mail: deposit@ccdc.cam.ac.uk].

Acknowledgments

Financial support by the European Union, allowing regular exchange of preliminary results with several European colleagues within the TOSS network under contract ERB-FMRX-CT980199, is gratefully acknowledged. Additional support by the ESF program Molecular Magnets is also kindly acknowledged. The work described in this paper has been supported by the Leiden University Study Group, WFMO, and has been performed under the aus-

pices of the Graduate Research School, HRSMC, a joint activity of Leiden University and the two Universities in Amsterdam. This work was also partly financially supported (A.L.S.) by the Council for the Chemical Sciences of the Netherlands Organization for Scientific Research (CW-NWO). Finally, financial support from the Materialwissenschaftliches Forschungszentrum der Universität Mainz and the Fonds der Chemischen Industrie is also gratefully acknowledged.

[1] P. Gütlich, A. Hauser, H. Spiering, *Angew. Chem. Int. Ed. Engl.* **1994**, 2024−2054.
[2] E. König, G. Ritter, S. K. Kulshreshtha, *Chem. Rev.* **1985**, 219−234.
[3] O. Kahn, C. J. Martinez, *Science* **1998**, *5347*, 44−48.
[4] P. Gütlich, in *Structure and Bonding* (Eds.: M. J. Clarke, P. Hemmerich, J. B. Goodenough, J. A. Ibers, C. K. Jørgensen, J. B. Neilands, D. Reiden, R. Weiss, R. J. P. Williams), Springer, Berlin, **1981**, p. 83−196.
[5] W. Vreugdenhil, J. H. van Diemen, R. A. G. de Graaff, J. G. Haasnoot, J. Reedijk, *Polyhedron* **1990**, *24*, 2971−2979.
[6] J. G. Vos, R. A. G. de Graaff, J. G. Haasnoot, A. M. van der Kraan, P. de Vaal, J. Reedijk, *Inorg. Chem.* **1994**, 2905−2910.
[7] W. Vreugdenhil, J. G. Haasnoot, O. Kahn, P. Thuéry, J. Reedijk, *J. Am. Chem. Soc.* **1987**, 5272−5273.
[8] G. Vos, R. A. le Fêbre, R. A. G. de Graaff, J. G. Haasnoot, J. Reedijk, *J. Am. Chem. Soc.* **1983**, 1682−1693.
[9] P. Stupik, J. H. Zhang, M. Kwiecien, W. M. Reiff, J. G. Haasnoot, R. Hage, J. Reedijk, *Hyperfine Interactions* **1986**, 725−727.
[10] P. Stupik, W. M. Reiff, R. Hage, J. Jacobs, J. G. Haasnoot, J. Reedijk, *Hyperfine Interactions* **1988**, 343−346.
[11] A. Ozarowski, Y. Shunzhong, B. R. McGarvey, A. Mislankar, J. E. Drake, *Inorg. Chem.* **1991**, 3167−3174.
[12] W. Vreugdenhil, S. Gorter, J. G. Haasnoot, J. Reedijk, *Polyhedron* **1985**, *10*, 1769−1775.
[13] O. Kahn, J. Krober, C. Jay, *Adv. Mater.* **1992**, *11*, 718−728.
[14] C. Jay, F. Grolière, O. Kahn, J. Kröber, *Mol. Cryst. Liq. Cryst.* **1993**, 255−262.
[15] J. Kröber, J. Audière, R. Claude, E. Codjovi, O. Kahn, J. G. Haasnoot, F. Grolière, C. Jay, A. Bousseksou, J. Linarès, F. Varret, A. Gonthier-Vassal, *Chem. Mater.* **1994**, 1404−1412.
[16] J. Kröber, E. Codjovi, O. Kahn, F. Grolière, C. Jay, *J. Am. Chem. Soc.* **1993**, 9810−9811.
[17] K. H. Sugiyarto, H. A. Goodwin, *Aust. J. Chem.* **1994**, 263−277.
[18] K. H. Sugiyarto, D. C. Craig, A. D. Rae, H. A. Goodwin, *Aust. J. Chem.* **1993**, 1269−1290.
[19] P. J. van Koningsbruggen, Y. Garcia, E. Codjovi, R. Lapouyade, O. Kahn, L. Fournès, L. Rabardel, *J. Mater. Chem.* **1997**, *10*, 2069−2075.
[20] Y. Garcia, P. J. van Koningsbruggen, G. Bravic, P. Guionneau, A. Chasseau, G. L. Cascarano, J. Moscovici, K. Lambert, A. Michalowicz, O. Kahn, *Inorg. Chem.* **1997**, 6357−6365.
[21] Y. Garcia, P. J. van Koningsbruggen, E. Codjovi, R. Lapouyade, O. Kahn, L. Rabardel, *J. Mater. Chem.* **1997**, *6*, 857−858.
[22] C. Cantin, H. Daubric, J. Kliava, Y. Servant, L. Sommier, O. Kahn, *J. Phys. Condens. Matt.* **1998**, *31*, 7057−7064.
[23] C. Janiak, T. G. Scharmann, J. C. Green, R. P. G. Parkin, M. J. Kolm, E. Riedel, W. Mickler, J. Elguero, R. M. Claramunt, D. Sanz, *Chem. Eur. J.* **1996**, *8*, 992−1000.
[24] K. H. Sugiyarto, D. C. Graig, A. D. Rae, H. A. Goodwin, *Aust. J. Chem.* **1994**, 869−890.
[25] E. Codjovi, L. Sommier, O. Kahn, C. Jay, *New J. Chem.* **1996**, *5*, 503−505.
[26] J. J. A. Kolnaar, G. van Dijk, H. Kooijman, A. L. Spek, V. G. Ksenofontov, P. Gütlich, J. G. Haasnoot, J. Reedijk, *Inorg. Chem.* **1997**, *11*, 2433−2440.
[27] J. J. A. Kolnaar, Ph.D. Thesis, Leiden University, **1998**.
[28] C. Janiak, T. G. Scharmann, T. Brauniger, J. Holubova, M. Nadvornik, *Z. Anorg. Allg. Chem.* **1998**, *5*, 769−774.
[29] A. Schreiner, Ph.D. thesis, University of Mainz **1995**.
[30] P. J. Kunkeler, P. J. van Koningsbruggen, J. P. Cornelissen, A. N. van der Horst, A. M. van der Kraan, A. L. Spek, J. G. Haasnoot, J. Reedijk, *J. Am. Chem. Soc.* **1996**, *9*, 2190−2197.
[31] K. H. Sugiyarto, D. C. Craig, A. D. Rae, H. A. Goodwin, *Aust. J. Chem.* **1995**, 35−54.
[32] R. Hage, Ph.D. Thesis, Leiden University, **1991**.
[33] A. L. Spek, *Acta Crystallogr.* **1990**, C34.
[34] P. Gütlich, R. Link, A. Trautwein, *Mössbauer Spectroscopy and Transition Metal Chemistry*, Springer, Berlin, **1978**.
[35] E. W. Müller, Ph.D. Thesis, University of Mainz, Germany, **1982**.
[36] H. Spiering, *EFFI Program for Mössbauer Spectra Fitting*, University of Mainz, Germany, **1999**.
[37] H. A. Goodwin, K. H. Sugiyarto, *Chem. Phys. Lett.* **1987**, *5*, 470−474.
[38] A. Hauser, *Chem. Phys. Lett.* **1986**, *6*, 543−548.
[39] G. Ritter, E. Konig, W. Irler, H. A. Goodwin, *Inorg. Chem.* **1978**, *2*, 225.
[40] C. P. Schlichter, H. G. Drickamer, *J. Chem. Phys.* **1972**, 2142.
[41] P. Gütlich, A. Hauser, H. Spiering, *Angew. Chem.* **1994**, 2109.
[42] O. Roubeau, A. F. Stassen, M. d. Vos, J. G. Haasnoot, J. Reedijk, to be published.
[43] R. Claude, J. Zarembowitch, M. Philoche-Levisalles, F. d'Yvoire, *New J. Chem.* **1991**, 625−641.
[44] R. Hernandez-Molina, A. Mederos, S. Dominguez, P. Gili, C. Ruiz-Perez, A. Castineiras, X. Solans, F. Lloret, J. A. Real, *Inorg. Chem.* **1998**, *20*, 5102−5108.
[45] R. Hage, J. G. Haasnoot, J. Reedijk, J. G. Vos, *Inorg. Chim. Acta* **1986**, 73−76.
[46] I. M. Kolthoff, P. J. Elving, *Treatise on Analytical Chemistry, Vol. 4*, New York, **1963**.
[47] M. Uda, Y. Hisazumi, K. Sato, S. Kubota, *Chem Pharm. Bull.* **1976**, *12*, 3103−3108.
[48] G. M. Sheldrick, *SHELXS-86: Program for crystal structure determination*, University of Göttingen, Germany, **1986**.
[49] G. M. Sheldrick, *SHELXL-97−2: Program for crystal structure refinement*, University of Göttingen, Germany, **1996**.
[50] A. J. C. Wilson, *International Tables for Crystallography, Volume C*, Kluwer Academic Publishers, Dordrecht, The Netherlands, **1992**.

Received February 18, 2000
[I00060]